Robustness Analysis and New Hybrid Algorithm of Wideband Source Localization for Acoustic Sensor Networks

Kun Yan, Hsiao-Chun Wu, *Senior Member, IEEE,* and S. S. Iyengar, *Fellow, IEEE*

Abstract—Wideband source localization using acoustic sensor networks has been drawing a lot of research interest recently in wireless communication applications, such as cellular handset localization, global positioning systems (GPS), and land navigation technologies, etc. The maximum-likelihood is the predominant objective which leads to a variety of source localization approaches. However, the appropriate optimization (search) algorithms are still being pursuit by researchers since different aspects about the effectiveness of such algorithms have to be addressed on different circumstances. In this paper, we focus on the two popular source localization methods for wideband acoustic signals, namely the alternating projection (AP) algorithm and the expectation maximization (EM) algorithm. We explore the respective limitations of these two methods and design a new hybrid approach thereupon. Through Monte Carlo simulations, we demonstrate that the trade-off can be achieved between the computational complexity and the localization accuracy using our newly proposed scheme. Moreover, we present the new robustness analysis for the source localization algorithms. We derive the Cramer-Rao lower bound (CRLB) involving the source spectral estimation error and thus prove that the new hybrid algorithm is more efficient than the EM algorithm. By employing the Gaussianity test, we also quantify the statistical mismatch between the actual statistics of the sensor signals and the underlying Gaussian model. We show that the Gaussianity measure can be a reliable robustness figure for source localization.

Index Terms—Source localization, alternating projection, expectation maximization, acoustic sensors, Gaussianity test, CRLB.

I. INTRODUCTION

S OURCE localization using low-cost and low-complexity sensor arrays has been the active research area in the fields of radar, sonar, geophysics, wireless communications and acoustic tracking for years [1]. Various techniques have been proposed for the narrow-band direction-of-arrival (DOA) estimation in the far field case [1]–[8]. Recently, the wideband source localization in the near field case has drawn a lot of research interest in the signal processing and communications applications [6]–[9]. Extensive studies for the wide-band

source localization can be found in [10]–[17]. Among them, the maximum-likelihood (ML) approach in [10] has been regarded as the optimal and robust scheme for coherent source signals. However, when the multiple sources are present, the ML approach poses a nonlinear optimization problem, which is impractical to solve especially for the energy-constrained sensor networks. Since the energy consumption is strictly limited in those sensor networks, the reduction in the computational complexity of the source localization algorithm appears to be crucial. Thus, the computational complexity issue remains challenging for the researchers in this area. Recently, we designed an Expectation-Maximization (EM) based localization algorithm for multiple wide-band sources [18] and it can be shown that our proposed algorithm is much more computationally efficient than the existing alternating projection (AP) method [10]–[17] for achieving the similar localization accuracy.

However, there are three major issues which have never been tackled in the existing literature regarding the source localization. First, the trade-off between the EM algorithm in [18] and the AP algorithm in [10]–[17] has not been studied in detail so far. Second, the comparative analysis based on the location estimation measures, such as Cramer-Rao lower bound (CRLB), has not been presented for the EM scheme versus the AP method. Third, the qualitative and quantitative justifications of the maximum-likelihood source location estimation using the Gaussian-mixture probabilistic model have never been addressed. Motivated by the aforementioned concerns, we make an attempt to answer these important questions in this paper.

Through our exhaustive heuristic studies, the EM source localization algorithm in [18] is rather sensitive to the initial condition since the EM based algorithms cannot guarantee that the global optimality would be achieved for any arbitrary initial condition. On the other hand, the AP source localization algorithm is based on the exhaustive search procedure, which certainly can reach the global optimality but the computational complexity would increase tremendously as the fine search-grid resolution is in demand. If the initial condition is ill-posed for the EM localization algorithm in [18], the AP algorithm in [10]–[17] can definitely perform better with a much larger computational complexity. In this paper, we will provide the computational complexity analyses of these two methods and propose a hybrid scheme to seek the trade-off between the accuracy and the complexity which are related to

the individual advantages of the two aforementioned source localization methods. In addition to the complexity analyses, we evaluate the robustness of these two localization schemes by deriving the corresponding CRLB. The effect of noise statistics will also be discussed [19]. Different noise characteristics will induce different probabilistic mismatchs between the actual statistics of the sensor signals and the underlying Gaussian-mixture model. We propose a new means to quantify this mismatch and show why the ML source localization performance varies with respect to different noise statistics.

The rest of this paper is organized as follows. The source localization problem formulation and the corresponding signal model are introduced in Section II. The maximum-likelihood objective function for the near-field wideband source localization is also derived in Section II. The associated alternating projection and expectation maximization algorithms to maximize this objective function are presented in Section III. The computational complexity analyses will be presented and a novel hybrid source localization algorithm will be proposed thereby in Section IV. The robustness analysis, which involves the CRLB derivation and the probabilistic mismatch evaluation, will be manifested in Section V. Monte Carlo simulation results for demonstrating our proposed new hybrid method and illustrating our newly derived robustness analysis will be provided in Section VI. Conclusion will be drawn in Section VII.

Nomenclature: $\underline{A}$ denotes a vector and $\widetilde{A}$ denotes a matrix. $\mathcal{C}$ and $\mathcal{R}$ denote the sets of complex and real numbers, respectively. $\widetilde{A}^T$, $\widetilde{A}^H$ are the transpose and the Hermitian adjoint of a matrix $\widetilde{A}$. The statistical expectation is denoted as $E\{\ \}$ and $\|\underline{A}\|$ denotes the Euclidean norm of the vector $\underline{A}$.

II. SIGNAL MODEL FOR SOURCE LOCALIZATION

According to [10], [20], we consider a randomly distributed array of P sensors to collect the data from M sources. Since the sources are assumed to be in the near field, the signal gains are different across the sensors. Thus, the signal collected by the pth sensor at time instant n is given by

$$x_p(n) = \sum_{m=1}^{M} a_p^{(m)} s_0^{(m)}\left(n - t_p^{(m)}\right) + w_p(n), \qquad (1)$$

for $n = 0, 1, \ldots, L-1$, $p = 1, \ldots, P$, $m = 1, \ldots, M$, where $a_p^{(m)}$ is the gain of the mth source signal arriving at the pth sensor; $s_0^{(m)}(n)$ denotes the mth source signal waveform; $t_p^{(m)}$ is the propagation delay (in data samples) incurred from the mth source to the pth sensor; $w_p(n)$ represents the zero-mean independently identically distributed (i.i.d.) noise process with variance σ^2. Several parameters can be specified as follows:

$t_p^{(m)} = \frac{\|\underline{r_s}^{(m)} - \underline{r_p}\|}{v}$: the propagation delay from the mth source to the pth sensor,

$\underline{r_s}^{(m)} \in \mathcal{R}^{2 \times 1}$: the mth source location,

$\underline{r_p} \in \mathcal{R}^{2 \times 1}$: the pth sensor location,

ν: the source signal propagation speed in meters/sec.

Taking the discrete Fourier transform (DFT) of both sides in Eq. (1), we have

$$\underline{X}(k) = \widetilde{D}(k)\underline{S_0}(k) + \underline{U}(k), \quad \text{for} \ \ k = 0, 1, \ldots, N-1, \quad (2)$$

where

$$\underline{X}(k) \stackrel{\text{def}}{=} [X_1(k) \ \cdots \ X_p(k)]^T \in \mathcal{C}^{P \times 1} \qquad (3)$$

and $X_p(k)$ is the kth DFT point of $x_p(n)$, $p = 1, \ldots, P$. The notations for the right-hand side of Eq. (2) are described as follows.

$$\widetilde{D}(k) \stackrel{\text{def}}{=} [\underline{d}^{(1)}(k) \ \cdots \ \underline{d}^{(M)}(k)] \in \mathcal{C}^{P \times M} \qquad (4)$$

consists of M *steering vectors*, each given by

$$\underline{d}^{(m)}(k) \stackrel{\text{def}}{=} [d_1^{(m)}(k) \ \cdots \ d_P^{(m)}(k)]^T \in \mathcal{C}^{P \times 1}, \ \ m = 1, \ldots, M, \qquad (5)$$

where

$$d_p^{(m)} \stackrel{\text{def}}{=} a_p^{(m)} e^{-\frac{j 2 \pi k t_p^{(m)}}{N}}, \qquad (6)$$

and $j \stackrel{\text{def}}{=} \sqrt{-1}$. Note that

$$\underline{S_0}(k) \stackrel{\text{def}}{=} [S_0^{(1)}(k) \ \cdots \ S_0^{(M)}(k)]^T \in \mathcal{C}^{M \times 1} \qquad (7)$$

consists of M individual source signal spectra, each given by $S_0^{(m)}(k)$ where $S_0^{(m)}(k)$ is the kth DFT point of $s_0^{(m)}(n)$, $m = 1, \ldots, M$.

In reality, the source signal spectral vector $\underline{S_0}(k)$ is unknown and deterministic. The noise spectral vector $\underline{U}(k) \in \mathcal{C}^{P \times 1}$ is a complex-valued zero-mean white Gaussian process and each element of $\underline{U}(k)$ has a variance $L\sigma^2$.

For source localization, we define the unknown parameter vector $\underline{\Theta} \in \mathcal{C}^{1 \times (MN + 2M)}$ as

$$\underline{\Theta} = \left[\underline{r_s}^T \ \underline{S_0}^{(1)^T} \ \cdots \ \underline{S_0}^{(m)^T} \ \cdots \ \underline{S_0}^{(M)^T} \right]^T, \qquad (8)$$

where

$$\underline{r_s} \stackrel{\text{def}}{=} \left[\underline{r_s}^{(1)^T} \ \cdots \ \underline{r_s}^{(m)^T} \ \cdots \ \underline{r_s}^{(M)^T} \right]^T \in \mathcal{R}^{2M \times 1}, \qquad (9)$$

and

$$\underline{S_0}^{(m)} \stackrel{\text{def}}{=} \left[S_0^{(m)}(0) \ \cdots \ S_0^{(m)}(N-1) \right]^T \in \mathcal{C}^{N \times 1}. \qquad (10)$$

According to Eqs. (2)-(10), we may construct the *equivalent log-likelihood* of the sensor signal spectra after neglecting the constant terms, which is given by

$$J(\underline{r_s}) = \log f_{\underline{X}} [\underline{\Theta}; \underline{X}(k)]$$
$$\stackrel{\text{def}}{=} - \sum_{k=0}^{N-1} \left[\underline{X}(k) - \widetilde{D}(k)\underline{S_0}(k) \right]^H \left[\underline{X}(k) - \widetilde{D}(k)\underline{S_0}(k) \right]. \qquad (11)$$

Thus, the maximum-likelihood estimation of $\underline{\Theta}$ can be achieved as

$$\hat{\underline{\Theta}} = \arg\max_{\underline{\Theta}} \left(J(\underline{r_s}) \right)$$
$$= \arg\min_{\underline{\Theta}} \left(\sum_{k=0}^{N-1} \left[\underline{X}(k) - \widetilde{D}(k)\underline{S_0}(k) \right]^H \right.$$
$$\left. \times \left[\underline{X}(k) - \widetilde{D}(k)\underline{S_0}(k) \right] \right). (12)$$

Eq. (12) yields the source signal spectral estimates $\hat{\underline{S_0}}(k)$ as

$$\hat{\underline{S_0}}(k) = \left(\widetilde{D}(k)^H \widetilde{D}(k) \right)^{-1} \widetilde{D}(k)^H \underline{X}(k), \ \ k = 0, 1, \ldots, N-1. \qquad (13)$$

According to [10] and Eqs. (11), (12), and (13), the ML source location estimates can be obtained as

$$\arg\max_{\underline{r_s}} \left(J(\underline{r_s})\right) = \arg\max_{\underline{r_s}} \left(\sum_{k=0}^{N-1} \left\| \widetilde{P}(k, \underline{r_s})\underline{X}(k) \right\|^2 \right),$$
(14)

where the *projection matrix* $\widetilde{P}(k, \underline{r_s}) \in \mathcal{C}^{P \times P}$ is defined as

$$\widetilde{P}(k, \underline{r_s}) \stackrel{\text{def}}{=} \widetilde{D}(k)\left(\widetilde{D}(k)^H \widetilde{D}(k)\right)^{-1}\widetilde{D}(k)^H.$$
(15)

For the single source case, the ML estimator in Eq. (14) can be further simplified as

$$\arg\max_{\underline{r_s}} \left(J(\underline{r_s})\right) = \arg\max_{\underline{r_s}} \left(\sum_{k=0}^{N-1} \left|B(k, \underline{r_s})\right|^2 \right),$$
(16)

where

$$B(k, \underline{r_s}) \stackrel{\text{def}}{=} \underline{d}(k, \underline{r_s})^H \underline{X}(k) = \underline{d}^{(1)}(k)^H \underline{X}(k)$$
(17)

is a scalar. Note that $\underline{d}^{(1)}(k)$ is a function of r_s implicitly according to Eqs. (1) and (2). It is obvious that the cost function $J(\underline{r_s})$ in Eq. (14) is nonlinear for multiple sources. Hence, the iterative methods are in demand for the associated optimization.

III. AP AND EM SOURCE LOCALIZATION ALGORITHMS

To solve Eq. (12) or Eq. (14), the AP schemes in [10]–[17] were proposed to decouple Eq. (14) into the single-source localization problems as described by Eq. (16) and then the exhaustive search procedure was applied to determine $\hat{\underline{\Theta}}$.

On the other hand, we can employ the EM-algorithm to solve Eq. (12) instead [18]. We define the *complete-data* as

$$\underline{X}^{(m)}(k) \stackrel{\text{def}}{=} \left[X_1^{(m)}(k)\ X_2^{(m)}(k)\ \cdots\ X_P^{(m)}(k)\right]^T \in \mathcal{C}^{P \times 1}$$
(18)

such that

$$\underline{X}(k) = \sum_{m=1}^{M} \underline{X}^{(m)}(k),$$
(19)

where $\underline{X}^{(m)}(k)$ denotes the mixture Gaussian process (with the cluster mean vector $\underline{d}^{(m)}(k)S_0^{(m)}(k)$ and the identical cluster covariance matrix $\frac{\sigma^2}{M}\widetilde{I}$, $\forall m$, and $\widetilde{I}$ is the $P \times P$ identity matrix) of the received signal spectrum contributed by the mth source. Thus, $\underline{X}(k)$ is defined as the *incomplete-data*.

Then Eq. (11) can be rewritten in terms of the complete data as

$$\log f_{\underline{X}}\left[\underline{\Theta}; \underline{X}^{(m)}(k)\right] \stackrel{\text{def}}{=}$$
$$- \sum_{m=1}^{M} \sum_{k=0}^{N-1} \left\| \underline{X}^{(m)}(k) - \underline{d}^{(m)}(k)S_0^{(m)}(k) \right\|^2, \quad (20)$$

and we define

$$f_{\underline{x}^{(m)}}\left(\underline{r_s}^{(m)}, \underline{S_0}^{(m)}\right) \stackrel{\text{def}}{=}$$
$$\sum_{k=0}^{N-1} \left\| \underline{X}^{(m)}(k) - \underline{d}^{(m)}(k)S_0^{(m)}(k) \right\|^2. \quad (21)$$

The log-likelihood of the complete data given by Eq. (20) is a summation of the individual log-likelihood functions for the incident sources given by $f_{\underline{x}^{(m)}}(\underline{r_s}^{(m)}, \underline{S_0}^{(m)})$ in Eq. (21). Thus, the source locations can easily be searched independently and separately using our proposed EM algorithm.

Since $\underline{X}^{(m)}(k)$, $m = 1, 2, \ldots, M$, are unknown, we have to estimate them based on $[\underline{X}(k), \hat{\underline{\Theta}}]$. Given the estimate $\hat{\underline{\Theta}}^{[i]}$ for the ith iteration ($i \geq 0$), the $(i+1)^{\text{th}}$ iteration of EM algorithm can be carried out thereby. Thus, the procedure is stated as follows. Calculate

$$Q(\hat{\underline{\Theta}}, \hat{\underline{\Theta}}^{[i]}) \stackrel{\text{def}}{=} E\left\{ \log f_{\underline{X}}\left[\underline{\Theta}; \underline{X}^{(m)}(k)\right] \middle| \underline{X}(k), \hat{\underline{\Theta}}^{[i]} \right\}$$
$$= \log f_{\underline{X}}\left[\hat{\underline{\Theta}}; \hat{\underline{X}}^{(m)}(k, \hat{\underline{\Theta}}^{[i]})\right],$$
$$\text{for}\quad m = 1, \ldots, M, \quad (22)$$

where

$$\hat{\underline{X}}^{(m)}(k, \hat{\underline{\Theta}}^{[i]}) \stackrel{\text{def}}{=} E\left[\underline{X}^{(m)}(k) \middle| \underline{X}(k), \hat{\underline{\Theta}}^{[i]}\right]$$
$$= \hat{\underline{d}}^{(m)}(k)\hat{S}_0^{(m)}(k) + \frac{1}{M}\left(\underline{X}(k) - \hat{\widetilde{D}}(k)\hat{\underline{S}_0}(k)\right).$$
(23)

It is noted that $\hat{\underline{d}}^{(m)}(k)$, $\hat{S}_0^{(m)}(k)$, $\hat{\widetilde{D}}(k)$, $\hat{\underline{S}_0}(k)$, $k = 0, 1, \ldots, N-1$, are all estimated using $\hat{\underline{r_s}}^{(m)}$ (the estimate of $\underline{r_s}^{(m)}$) obtained from the previous iteration i according to the definitions given by Eqs. (4), (5), (6), (7) and (10).

Then, re-estimate $\underline{\Theta}$ by maximizing $\log f_{\underline{X}}\left[\hat{\underline{\Theta}}; \hat{\underline{X}}^{(m)}(k, \hat{\underline{\Theta}}^{[i]})\right]$ in Eq. (22) as

$$\hat{\underline{\Theta}}^{[i+1]} = \arg\max_{\underline{\Theta}} \left\{ \log f_{\underline{X}}\left[\hat{\underline{\Theta}}; \hat{\underline{X}}^{(m)}(k, \hat{\underline{\Theta}}^{[i]})\right] \right\}.$$
(24)

The solution to Eq. (24) is

$$\hat{\underline{r_s}}^{(m)} = \arg\max_{\underline{r_s}^{(m)}} \sum_{k=0}^{N-1} \left| \left[\hat{\underline{d}}^{(m)}(k)\right]^H \hat{\underline{X}}^{(m)}(k, \hat{\underline{\Theta}}^{[i]}) \right|^2$$
$$= \arg\max_{\underline{r_s}^{(m)}} \sum_{k=0}^{N-1} |\Upsilon_i|^2, \quad (25)$$

where

$$\Upsilon_i \stackrel{\text{def}}{=} \left[\hat{\underline{d}}^{(m)}(k)\right]^H \hat{\underline{X}}^{(m)}(k, \hat{\underline{\Theta}}^{[i]}),$$
(26)

and

$$\hat{S}_0^{(m)}(k) = \frac{\left[\hat{\underline{d}}^{(m)}(k)\right]^H \hat{\underline{X}}^{(m)}\left(k, \hat{\underline{\Theta}}^{[i]}\right)}{\left\| \hat{\underline{d}}^{(m)}(k) \right\|^2},$$
(27)

for $m = 0, 1, \ldots, M$, $k = 0, 1, \ldots, N-1$. Then update

$$\hat{\underline{\Theta}}^{[i+1]} = \left[\hat{\underline{r_s}}^T\ \hat{\underline{S}_0}^{(1)^T}\ \cdots\ \hat{\underline{S}_0}^{(m)^T}\ \cdots\ \hat{\underline{S}_0}^{(M)^T}\right]^T,$$
(28)

where

$$\hat{\underline{r_s}} \stackrel{\text{def}}{=} \left[\hat{\underline{r_s}}^{(1)^T}\ \cdots\ \hat{\underline{r_s}}^{(m)^T}\ \cdots\ \hat{\underline{r_s}}^{(M)^T}\right]^T,$$
(29)

and

$$\hat{\underline{S}_0}^{(m)} \stackrel{\text{def}}{=} \left[\hat{S}_0^{(m)}(0)\ \cdots\ \hat{S}_0^{(m)}(N-1)\right]^T,$$
$$\text{for}\quad m = 1, \ldots, M. \quad (30)$$

The E- and M-steps are repeated until the pre-defined convergence of the estimated parameters is achieved.

IV. COMPUTATIONAL COMPLEXITY STUDIES AND NOVEL HYBRID SOURCE LOCALIZATION SCHEME

There is a trade-off between the localization accuracy and the computational complexity when the aforementioned AP and EM algorithms are adopted. The studies of computational complexity for these two source localization algorithms are presented in the following subsections.

A. Computational Complexities for Complex Multiplications

For simplicity, in our computational complexity studies of the AP and EM source localization schemes, we only consider the computational burden for complex multiplications. In addition, the computations of the discrete Fourier transform and the matrices $\widetilde{D}(k)$, $k = 0, 1, \ldots, N - 1$, are neglected. N_x, N_y denote the numbers of search points along the $x-$ and $y-$axes, respectively. For our proposed EM method, we need NM^2P^3 complex multiplications to carry out Eq. (23), $NN_xN_yMP^2$ multiplications to carry out $\sum_{k=0}^{N-1} |\Upsilon_i|^2$ in Eq. (25), and NMP complex multiplications to carry out $\frac{\left[\hat{\underline{d}}^{(m)}(k)\right]^H \hat{X}^{(m)}\left(k, \hat{\underline{\Theta}}^{[i]}\right)}{\|\hat{\underline{d}}^{(m)}(k)\|^2}$ in Eq. (27). Consequently, in our proposed EM algorithm, the number of complex multiplications per iteration is

$$\mathbb{C}_{\text{EM}}^{\times}(N, M, P, N_x, N_y) = N\left(M^2P^3 + MP + N_xN_yMP^2\right). \tag{31}$$

According to [10], it is easy to derive the number of complex multiplications for the existing AP method as

$$\mathbb{C}_{\text{AP}}^{\times}(N, M, P, N_x, N_y) = NM^2P^3N_xN_y. \tag{32}$$

B. Computational Complexities for Comparison Operations

Furthermore, the search for the maximum objective function values is needed by both AP and EM schemes. There involve $N_xN_y - 1$ comparison operations in Eq. (25) for each source per iteration in our proposed EM algorithm. Thus we need $M\zeta(N_xN_y - 1)$ comparison operations where ζ is the total iteration number and M is the source number. For the AP method, we need $M\zeta(N_xN_y - 1)$ comparison operations (ζ iterations for the AP method are also assumed for a fair comparison). Since the EM algorithm for each source location estimate can be carried out in parallel, we actually need to undertake $\zeta(N_xN_y - 1)$ comparison operations per computer. The AP algorithm has to do the maximum search for each source location estimate sequentially instead (impossible for parallel computation) [10]. Hence, the numbers of comparison operations needed by these two methods are

$$\mathbb{C}_{\text{EM}}^{com} = \zeta(N_xN_y - 1) \tag{33}$$

and

$$\mathbb{C}_{\text{AP}}^{com} = M\zeta(N_xN_y - 1). \tag{34}$$

According to Eqs. (33) and (34), the EM method requires only $\frac{1}{M}$ times of the comparison operations as many as the AP method if the parallel computation is feasible. However, the EM method is very sensitive to the initial condition and can only assure the sub-optimality.

C. Novel Hybrid Source Localization Algorithm

From the previous discussion in Sections III, IV-A and IV-B, the obvious trade-off is inevitably encountered between the AP and the EM methods in practice. To seek the best trade-off between the localization performance and the incurred computational complexity, we propose a new hybrid source localization scheme as follows:

Step 1) Employ the AP algorithm using the "rough" resolution, which is specified by N_x', N_y' grid points in the x- and y-directions, respectively. The outcome of this step can be considered as the coarse location estimate $\underline{r_S}'$.

Step 2) Utilize the estimation outcome $\underline{r_S}'$ from Step 1 to carry out the EM procedure with a finer resolution, which is specified by the new grid parameters N_x'', N_y'' for ζ iterations. The ultimate location estimate can be achieved as $\underline{r_S}''$.

It is obvious that the computational complexity $\mathbb{C}_{Hybrid}^{\times}$ for the above-described new hybrid source localization scheme in terms of complex multiplications can be expressed as

$$\begin{aligned} \mathbb{C}_{Hybrid}^{\times} &= \mathbb{C}_{\text{AP}}^{\times}(N, M, P, N_x', N_y') \\ &+ \zeta\, \mathbb{C}_{\text{EM}}^{\times}(N, M, P, N_x'', N_y''). \end{aligned} \tag{35}$$

According to Eqs (31)-(34), the trade-off between the computational complexity and the location estimation accuracy can be maneuvered. Our new hybrid method would be much less sensitive to the initial condition than our previously proposed EM algorithm [18] but it also leads to a much less computational complexity than the conventional AP method [10]–[17].

V. ROBUSTNESS ANALYSIS FOR SOURCE LOCALIZATION ALGORITHMS

To evaluate our novel hybrid source localization scheme, we provide the Cramer-Rao Lower Bound (CRLB) of the source location estimator. By analyzing the CRLB, we prove that our proposed hybrid algorithm is more robust than the EM algorithm in [18]. The major factor is the probabilistic mismatch. In this section, we will employ the Non-Gaussianity test for source localization to demonstrate that the source localization estimator is sensitive to the mismatch between the adopted underlying statistical model (Gaussian mixture) and the actual sensor signal statistics.

A. Cramer-Rao Lower Bound for Source Location Estimation

To study the robustness, we first derive the CRLB involving the source spectral estimation here. The source spectral estimation error $\underline{\varepsilon}(k)$, $k = 0, 1, \ldots, N - 1$, is defined as

$$\underline{\varepsilon}(k) \overset{\text{def}}{=} \underline{\hat{S}}_0(k) - \underline{S}_0(k), \quad \text{for} \ \ k = 0, 1, \ldots, N - 1, \tag{36}$$

where $\hat{S}_0^{(m)}(k) = S_0^{(m)}(k) + \varepsilon^{(m)}(k)$, $m = 1, \ldots, M$ denotes the source signal spectral estimate. We define

$$\underline{\lambda_p}^{(m)} \overset{\text{def}}{=} \frac{\hat{\underline{r_s}}^{(m)^T} - \underline{r_p}^T}{\|\hat{\underline{r_s}}^{(m)} - \underline{r_p}\|} \in \mathcal{R}^{1\times 2}, \tag{37}$$

where $\hat{\underline{r_s}}^{(m)}$ is given by Eq. (25) and $\underline{r_p}$ is defined below Eq. (1). Given the signal model as described in Section II, we

derive the entries in *Fisher information matrix* $\widetilde{\mathcal{F}} \in \mathcal{R}^{2M \times 2M}$ for the source location vector $\underline{r}_s$ as (according to [21])

$$
\begin{aligned}
\widetilde{\mathcal{F}}(m_1, m_2) =& \frac{4\pi^2}{LN^2\sigma^2 \upsilon^2} \\
& \times \sum_{p=1}^{P} \left(a_p^{(m_1)} a_p^{(m_2)} \exp\left[-\frac{j2\pi\left(t_p^{(m_2)} - t_p^{(m_1)}\right)}{N} \right] \right. \\
& \left. \times E\left\{ \underline{\lambda_p}^{(m_1)^T} \underline{\lambda_p}^{(m_2)} \right\} \right) E\left\{ \hat{S}_0^{(m_1)^H}(k)\, \hat{S}_0^{(m_2)}(k) \right\}.
\end{aligned}
\tag{38}
$$

Considering the source spectral estimation error defined by Eq. (36), we get

$$
\begin{aligned}
\widetilde{\mathcal{F}}(m_1, m_2) =& \frac{4\pi^2}{LN^2\sigma^2 \upsilon^2} \\
& \times \sum_{p=1}^{P} \left(a_p^{(m_1)} a_p^{(m_2)} \exp\left[-\frac{j2\pi\left(t_p^{(m_2)} - t_p^{(m_1)}\right)}{N} \right] \right. \\
& \left. \times E\left\{ \underline{\lambda_p}^{(m_1)^T} \underline{\lambda_p}^{(m_2)} \right\} \right) \\
& \times \left[S_0^{(m_1)^H}(k) S_0^{(m_2)}(k) + E\left\{ \varepsilon^{(m_1)^H}(k)\varepsilon^{(m_2)}(k) \right\} \right. \\
& \left. + S_0^{(m_1)^H}(k) E\left\{ \varepsilon^{(m_2)}(k) \right\} + S_0^{(m_2)}(k) E\left\{ \varepsilon^{(m_1)^H}(k) \right\} \right],
\end{aligned}
\tag{39}
$$

where m_1, m_2 indicate the associated row and column indices, respectively. According to Eq. (58) in the appendix, we get

$$
E\left[(\hat{\underline{r}}_s - \underline{r}_s)^2 \right] \geq tr\left[\widetilde{\mathcal{F}}^{-1} \right],
\tag{40}
$$

where $tr\left[\widetilde{\mathcal{F}}^{-1} \right]$ is the CRLB and $tr[\ \ ]$ is the trace of a square matrix. According to Eqs. (39) and (40), it is obvious that the estimation error $\underline{\varepsilon}(k)$ will affect the CRLB. Since the EM algorithm initializes randomly, such initial location errors are bounded as

$$
E\left[(\hat{\underline{r}}_s - \underline{r}_s)^2 \right] \leq \frac{M}{2}\left((\ell_x)^2 + (\ell_y)^2 \right),
\tag{41}
$$

where ℓ_x and ℓ_y correspond to the lateral sizes of the x- and y-directions, respectively, for the entire search scope. On the other hand, since our novel hybrid algorithm as presented in Section IV-C is initialized using the AP algorithm [10]–[17] with a rougher resolution, the corresponding estimation error of the source location vector is bounded as

$$
E\left[(\hat{\underline{r}}_s - \underline{r}_s)^2 \right] \leq \frac{M}{2}\left(\left(\frac{\ell_x}{N_x'}\right)^2 + \left(\frac{\ell_y}{N_y'}\right)^2 \right).
\tag{42}
$$

It is well known that the EM algorithm is sensitive to the initial location [18]. Obviously our proposed hybrid algorithm in Section IV-C would lead to a smaller estimation error $E\left[(\hat{\underline{r}}_s - \underline{r}_s)^2 \right]$ than the EM algorithm with random initialization [18].

B. Non-Gaussianity Test

The ML source localization as introduced in Section II relies on the multivariate mixture Gaussian density (or Gaussian mixture) model. However this assumption is not valid in general especially when the signal sample size is limited and the signal-to-noise (SNR) is large [22]. According to [10], the received signals at the sensor array are always modeled as a Gaussian mixture. Since the source spectra $\underline{S}_0(k)$ are not necessarily Gaussian, the statistical mismatch would occur frequently thereby.

After numerous simulations, we have discovered a very interesting fact as follows. Consider that the source localization is performed in two cases for the same source signals at the same comparative SNR, namely when the ambient noise is uniformly distributed and when the ambient noise is Gaussianly distributed. The former performance is better than the latter according to our heuristic studies. To explain this phenomenon, we employ the Gaussianity test for the received signals added with these two different kinds of ambient noise. Since the ML location estimation relies on the DFT, the Gaussianity measure has to be undertaken on the DFT sequences.

The received signal spectral waveform at the pth sensor is given by

$$
\begin{aligned}
X_p(k) &= \mathbf{Re}\{X_p(k)\} + \sqrt{-1}\ \mathbf{Im}\{X_p(k)\} \\
&= \sum_{n=0}^{N-1}\left[\cos\left(\frac{2\pi kn}{N}\right) x(n) \right. \\
&\quad \left. + \sqrt{-1} \sum_{n=0}^{N-1} \sin\left(\frac{2\pi kn}{N}\right) x(n) \right], \\
&\qquad\qquad k = 0, 1, \ldots, N-1.
\end{aligned}
\tag{43}
$$

According to Eq. (43), we can measure the Gaussianities separately for the real and imaginary parts of $X_p(k)$. The relevant statistical characterization approaches are discussed in the following subsections.

1) Edgeworth Expansion for PDF Characterization: As previously stated, the finite sample size and high SNR would often lead to the non-Gaussian characteristics of the received signals [22]. We use the Edgeworth expansion to model the actual statistics of the aforementioned signal $\mathbf{Re}\{X_p(k)\}$ and evaluate the mismatch between the actual statistics and the underlying Gaussian mixture model [23], [24]. Similar to the Gram-Charlier series, the Edgeworth expansion can be used to characterize the unknown probability density function (PDF) based on the moments and the cumulants.

For a random variable Z ($Z = \mathbf{Re}\{X_p(k)\}$ in our application here) with $E\{Z\} = 0$ (this can always be achieved by setting a new random variable Z as $Z - E\{Z\}$) and unit variance for simplicity, the arbitrary probability density function for Z can be written by the Edgeworth expansion as [23], [24]:

$$
f_Z(z) = \vartheta(z)\left\{ 1 + \sum_{k=1}^{+\infty} P_k(z) \right\},
\tag{44}
$$

where $\vartheta(z)$ is the zero-mean univariate Gaussian PDF, which

is given by

$$\vartheta(z) \overset{\text{def}}{=} \frac{1}{\sqrt{2\pi}} \exp\left(-\frac{z^2}{2}\right), \qquad (45)$$

and $P_k(z)$ is a polynomial such that

$$P_k(z) \overset{\text{def}}{=} \sum_{\{l_m\}} H_{k+2\varpi}(z) \prod_{m=1}^{k} \frac{1}{l_m!} \left(\frac{\chi_{m+2}}{(m+2)!}\right)^{l_m}. \qquad (46)$$

Here the set $\{l_m\}$ consists of all non-negative integer solutions to the equation $l_1 + 2l_2 + \ldots + kl_k = k$, and $\varpi = l_1 + l_2 + \ldots + l_k$. Note that χ_l is the lth-order cumulant of $Z = \mathbf{Re}\{X_p(k)\}$, which is given by

$$\chi_l = (-1)^l \frac{d^l}{d\eta^l} \log \hat{f}_Z(\eta) \mid_{\eta=0}, \qquad (47)$$

where $\hat{f}_Z(\eta) \overset{\text{def}}{=} E\{e^{jz\eta}\}$ is the characteristic function of $Z = \mathbf{Re}\{X_p(k)\}$ and $H_l(z)$ is the lth-order Hermite polynomial such that

$$\vartheta(z) H_l(z) = (-1)^l \frac{d^l}{dz^l} \vartheta(z). \qquad (48)$$

2) Gaussianity Measure Using Bispectrum: The Edgeworth expansion in Eq. (44) cannot provide the specific measurement of the aforementioned mismatch. Instead, the Gaussianity measure based on the bispectrum can be employed to examine the statistics for time series [25]. If $z(0), z(1), \ldots, z(N-1)$ is the sensor signal sequence ($z(n) = x_p(n)$, for any p), its bispectrum is defined as

$$\hat{C}_{zzz}(i', i'') \overset{\text{def}}{=} \frac{1}{N} Z(i') Z(i'') Z^H(i' + i''), \qquad (49)$$

where $Z(i') = \sum_{n=0}^{N-1} z(n) \exp\left(\frac{-j2\pi ni'}{N}\right)$ is the N-point discrete Fourier transform of the signal $z(0), z(1), \ldots, z(N-1)$. The estimated bispectrum can be further smoothed by a two-dimensional window $W(i', i''), 0 \leq i', i'' \leq \mathbf{M}_w - 1$, (window size is $\mathbf{M}_w \times \mathbf{M}_w$) [25]. Then a sampled bispectrum is used to construct a statistical test whether the bispectrum given by Eq. (49) is nonzero; whereas a rejection action of the null hypothesis implies that the signal is Gaussian [25]. The statistics is constructed below. According to Eq. (49), we can compute

$$\zeta_{i', i''} = \frac{\hat{C}_{zzz}(i', i'')}{\sqrt{\frac{N}{\mathbf{M}_w^2}\left(\hat{S}_{zz}(i')\hat{S}_{zz}(i'')\hat{S}_{zz}(i' + i'')\right)}}. \qquad (50)$$

It is noted that $\zeta_{i', i''}$ is random according to Eq. (50). It can be proved that the PDF of $\zeta_{i', i''}$ is complex Gaussian with unit-variance [25], [26]. Here $\hat{S}_{zz}(i')$ is the sample estimate for the power spectrum of $z(0), z(1), \ldots, z(N-1)$. Consequently, $|\zeta_{i', i''}|^2$ is approximately a chi-square random variable with two degrees of freedom. Thus, we can construct the statistics Φ for the Gaussianity test [25], [26]:

$$\Phi \overset{\text{def}}{=} 2 \sum_{i'=0}^{N-1} \sum_{i''=0}^{N-1} |\zeta_{i', i''}|^2. \qquad (51)$$

Asymptotically speaking, Φ is chi-square distributed under the null hypothesis of Gaussianity. Hence it is easy to derive a statistical test to determine whether the observation is consistent

with a central chi-squared distribution; this "consistency" is characterized as the *probability-of-false-alarm* value, i.e. the probability that the sensor data possess a nonzero bispectrum. If this *probability-of-false-alarm* value is small, we can get a higher probability of accepting the Gaussian assumption.

Since the sample size is limited in source localization, we cannot directly apply the technique in [25] (it requires a large sample size) to estimate the bispectrum of the sensor signal. Instead, we use the bootstrap algorithm which is more appropriate for finite sample sizes [26]. The estimation result within a primary region is considered only due to the symmetry of the bispectrum such that

$$D \overset{\text{def}}{=} \left\{0 < i' \leq \frac{N}{2}, 0 < i'' < i', 2i' + i'' < N\right\}. \qquad (52)$$

We propose to use the Gaussianity test, as given by Eq. (51), for the robustness analysis of the ML source localization. The application of this new analysis can be manifested in the next section.

VI. SIMULATION

In this section, we provide the simulation results for our proposed hybrid source localization scheme in Section IV-C and our new robustness analysis in Section V. We present the comparison of the three underlying schemes, namely (1) the conventional alternating projection method (AP), (2) our previously proposed EM method (EM) and (3) the novel hybrid method (AP-EM hybrid). Acoustic source signal is acquired from [10]. The sampling frequency is 100 kHz. The propagation speed is 345 meter/sec. The data is simulated for a circularly-shaped array of five sensors using the recorded acoustic data from [10]. The sample size is $L = 200$ and the DFT size is $N = 256$. Two-dimensional grid-point search is employed in the scope of 10 meters by 10 meters, where both x- and y- axes are uniformly sampled. Fifty Monte Carlo experiments are carried out. In the EM algorithm, randomly initiated source locations are used for a particular signal-to-noise ratio (SNR=20 dB).

The resolution parameters are chosen as $N_x = N_y = 100$ for both AP and EM methods. On the other hand, for the new hybrid scheme, the resolution parameters are chosen as $N_x' = N_y' = 5$ for Step 1 and $N_x'' = N_y'' = 100$ for Step 2, respectively. The iteration number ζ is 5 for both EM and AP-EM hybrid schemes. Figure 1 depicts the *average root-mean-square errors* versus different signal-to-noise ratios (SNRs). It can be observed in Figure 1 that our proposed hybrid method almost always achieves the highest accuracy (lowest RMS errors) among the three schemes in comparison. The detailed accuracy performances are illustrated in Table I for the individual source location estimates. We also delineate the computational complexity curves versus the numbers of sources, M, in Figure 2. Our newly proposed hybrid scheme leads to a much less complexity than the conventional AP method as illustrated in Figure 2. The computational complexity of the hybrid scheme is very close to that of the EM algorithm. To visualize the trade-off between the computational complexity and the estimation accuracy (RMS error), we propose to enumerate the product between them. Figure 3 depicts the *trade-off* curve (the product of the computational
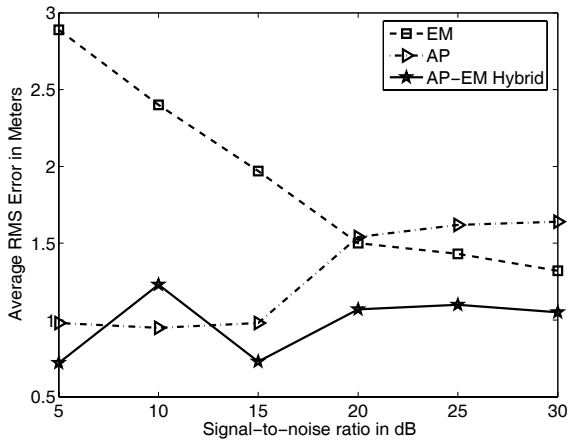
Fig. 1.   Average root-mean-square (RMS) errors versus SNR.
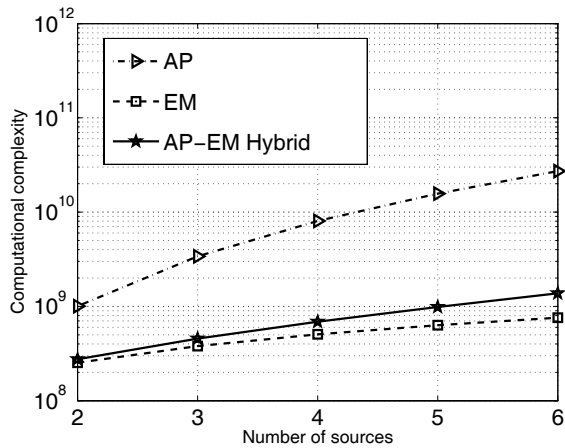
Fig. 2.   The computational complexity in terms of complex multiplications versus the number of sources for the three compared schemes.

Fig. 3.   The trade-off curves (product of computational complexity and summed root-mean-square error for both sources) versus signal-to-noise ratio (SNR).
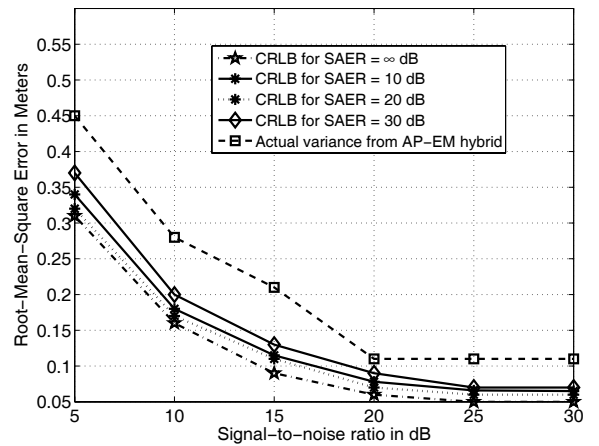
Fig. 4.   Cramer-Rao lower bounds for different SAER values (10, 20, 30 dB, error-free or ∞ dB) and the actual source location estimation variance resulting from our proposed AP-EM hybrid algorithm versus the signal-to-noise ratio.

complexity and the RMS error) versus the SNRs for these three methods.

For the robustness analysis of source localization, we use the derived CRLB to illustrate the optimistic estimation variance. The CRLBs are demonstrated in Figure 4. The *signal-to-approximation-error ratio* (SAER), which is a critical factor controlling the CRLB, is given by

$$SAER \overset{\text{def}}{=}$$
$$\frac{1}{N} \sum_{k=0}^{N-1} \left(10 \log_{10} \left[\frac{E\left\{ \sum_{m=1}^{M} \left| S_0^{(m)}(k) \right|^2 \right\}}{E\left\{ \sum_{m=1}^{M} \left| \varepsilon^{(m)}(k) \right|^2 \right\}} \right] \right) \quad (53)$$

Obviously, a reliable source spectral estimate ($|\varepsilon^{(m)}(k)|$ is small) leads to a large SAER, definitely improves the source localization performance and results in a smaller CRLB.

To provide some insight of the reason why our proposed hybrid algorithm is more robust than the EM algorithm, we calculate the spectral estimation error for the first iteration of the EM algorithm and the spectral estimation error for the first iteration of the new hybrid algorithm after the rough-resolution initialization with the help of the AP method as

described in Section III. Figure 5 depicts the average spectral estimation error $(1/N) \sum_{k=0}^{N-1} E\left\{ \sum_{m=1}^{M} |\varepsilon^{(m)}(k)|^2 \right\}$, $m = 1, 2$, over 100 Monte Carlo trials versus the SNR. Clearly, the EM algorithm leads to larger average spectral estimation errors and therefore it also induces larger CRLBs since the EM algorithm is sensitive to the random initialization.

Using the Gaussianity test, we can quantify the statistical mismatch for source localization and develop the corresponding robustness analysis. Three kinds of noise are artificially added to the acoustic data from [10]. The localization performances in terms of average RMS errors are depicted in Figures 6 for uniform, Laplace and Gaussian noises, respectively. The detailed accuracy performances are illustrated in Table II for the individual source location estimates. Surprisingly, the localization results based on uniform noise outperform the others. This phenomenon is caused by the statistical mismatch. When the sample size is limited and the SNR is large, the Gaussian model cannot fit the sensor data perfectly. To visu-

TABLE I
AVERAGE ROOT-MEAN-SQUARE (RMS) ERRORS IN METERS FOR THE LOCATION ESTIMATES OF SOURCES 1 AND 2

SNR (dB)	5	10	15	20	25	30	Average
EM (source 1)	3.47	2.69	2.37	1.97	1.86	1.77	2.36
EM (source 2)	2.09	2.06	1.50	0.88	0.78	0.68	1.33
AP (source 1)	1.29	1.25	1.29	2.53	2.54	2.50	1.90
AP (source 2)	0.54	0.47	0.54	0.45	0.45	0.45	0.48
AP-EM hybrid (source 1)	1.17	1.82	1.19	1.83	1.96	1.81	1.63
AP-EM hybrid (source 2)	0.48	0.42	0.16	0.15	0.16	0.22	0.27
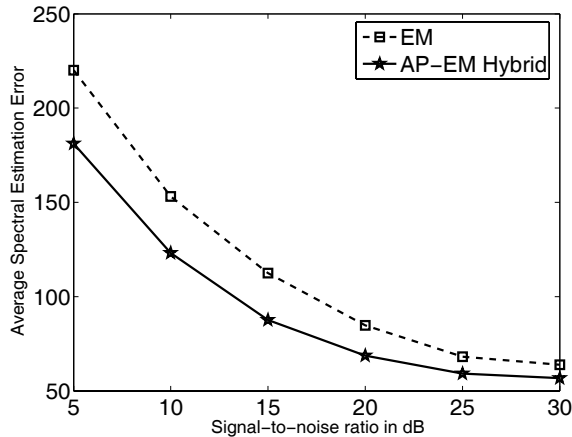
Fig. 5. Average spectral estimation errors $E\left\{\sum_{m=1}^{M}|\varepsilon(k)|^2\right\}$ resulting from the EM algorithm and the hybrid algorithm over 100 Monte Carlo experiments.
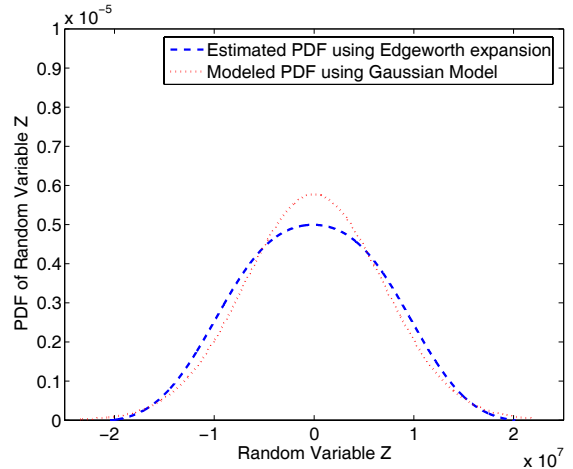
Fig. 7. The actual PDF resulting from the Edgeworth expansion and the PDF using the underlying Gaussian model for the sensor signal of finite sample size.
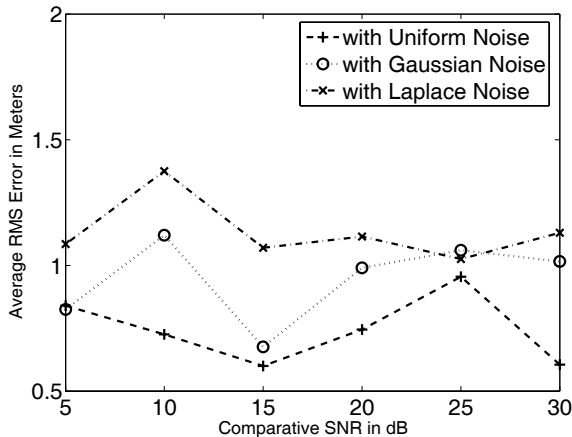
Fig. 6. Average root-mean-square (RMS) error versus comparative SNR for the source localization with different noise models. The comparative SNR is the average SNR over all the sensor signals.

alize this mismatch, an Edgeworth expansion is employed to generate the "actual" PDF while an underlying Gaussian PDF is also generated using the estimates of mean and variance from the sensor data for comparison. These two PDFs are plotted in Figure 7 and the obvious discrepancy can be found therein.

Moreover, to demonstrate our newly derived robustness analysis, we apply the Gaussian rejection hypothesis in [25] for the two sensor signal sets used to generate Figure 6. Figure 8 depicts the probabilities of rejection (as stated in

Section V) for the aforementioned data added with either Gaussian (denoted as "with Gaussian Noise" in the figure), Laplace (denoted as "with Laplace Noise" in the figure) or uniform noise (denoted as "with Uniform Noise" in the figure). According to Figure 8, the interesting result can be found that the sensor data involving the uniform noise is "more Gaussian" than that involving the Gaussian noise. Hence the former leads to a less statistical mismatch and thus outperforms the latter in source localization. The CRLB we deduced in Section V-A is also used to compare different noise statistics. We artificially add the signal with generalized Gaussian noises (possessing different kurtosis values) [27] and the CRLBs corresponding to these different noise statistics are compared in Figure 9 for three different SNRs. It is obvious that the CRLB decreases with the increase in the kurtosis value.

VII. CONCLUSION

In this paper, we investigate the AP and EM algorithms for multiple wide-band source localization and make an attempt to seek the trade-off between the computational complexity and the localization accuracy. Through the analysis and the empirical studies for the AP and EM source localization methods, we design a new multi-resolution hybrid source localization scheme to overcome their individual disadvantages. The Monte Carlo simulation results show that our proposed hybrid scheme can outperform both AP and EM methods in terms of the accuracy and the corresponding trade-off measure (the product of complexity and accuracy). This new hybrid scheme turns out to be optimal among these three methods

TABLE II
AVERAGE ROOT-MEAN-SQUARE (RMS) ERRORS IN METERS FOR THE LOCATION ESTIMATES OF DIFFERENT NOISE STATISTICS

SNR (dB)	5	10	15	20	25	30	Average
AP-EM with Gaussian Noise (source 1)	1.17	1.82	1.19	1.83	1.96	1.81	1.63
AP-EM with Uniform Noise (source 1)	1.34	1.20	1.0	1.40	1.79	0.98	1.29
AP-EM with Laplacian Noise (source 1)	1.60	2.02	1.80	1.95	1.75	1.94	1.84
AP-EM with Gaussian Noise (source 2)	0.48	0.42	0.16	0.15	0.16	0.22	0.27
AP-EM with Uniform Noise (source 2)	0.34	0.25	0.20	0.09	0.12	0.23	0.21
AP-EM with Laplacian Noise (source 2)	0.97	0.73	0.34	0.28	0.30	0.32	0.42
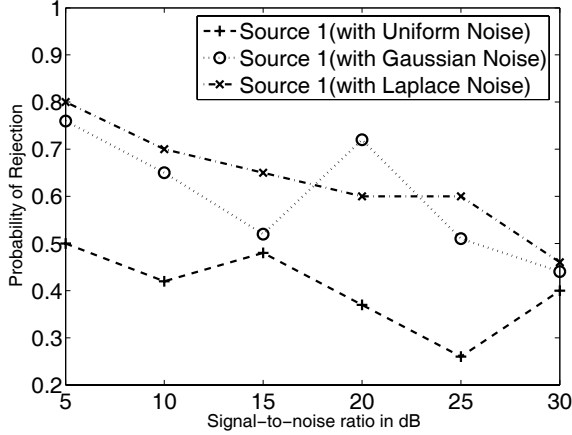
Fig. 8. Probabilities of rejection versus SNR for three different sets of sensor signals (Source 1) enduring Gaussian, uniform and Laplace noises.
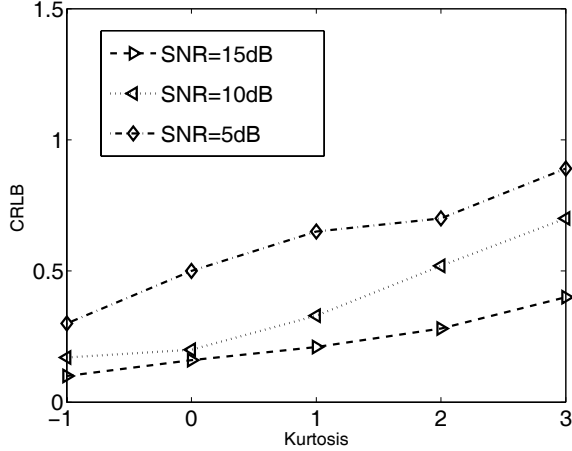
Fig. 9. CRLB with respect to different noise statistics in terms of kurtosis. Kurtosis of a mean-removed random variable Y, i.e., $E\{Y\} = 0$, is defined as $\frac{E\{|Y|^4\}}{E^2\{|Y|^2\}} - 3$.

in such a sense. To provide the robustness analysis for source localization algorithms, we derive the CRLB of the source localization problem. Finally, we discuss the influence of the statistical mismatch on the source localization algorithms. Using the Edgeworth expansion and the bispectrum, we can measure the departure of Gaussianity for different sensor signals or the received signals enduring different kinds of ambient noise. By employment of the Gaussianity test for the sensor signals, we can quantify the statistical mismatch and provide the corresponding robustness figures.

APPENDIX

In this appendix, we derive the CRLB based on the signal model in Eq. (2) with the estimated received signal spectrum $\left[\underline{\hat{S}_0}^{(1)^T}, \ldots, \underline{\hat{S}_0}^{(m)^T}, \ldots, \underline{\hat{S}_0}^{(M)^T}\right] \in \mathcal{C}^{1 \times MN}$, where $\underline{\hat{S}_0}^{(m)}$ is defined in Eq. (30). The parameters for the CRLB derivation are $\underline{r_s}^T = \left[\underline{r_s}^{(1)^T} \cdots \underline{r_s}^{(m)^T} \cdots \underline{r_s}^{(M)^T}\right] \in \mathcal{R}^{1 \times 2M}$, where $\underline{r_s}^{(m)^T} \overset{\text{def}}{=} [x_s^{(m)}, y_s^{(m)}]$. Note that $x_s^{(m)}, y_s^{(m)}$ are the $x-$ and $y-$ coordinates of source m, respectively. Since the PDF of the received signal is multivariate Gaussian, the Fisher information matrix $\widetilde{\mathcal{F}} \in \mathcal{R}^{2M \times 2M}$ of $\underline{r_s}^T$ is given by

$$\widetilde{\mathcal{F}} = E\left\{\left(\frac{\partial(\widetilde{D}(k)\underline{\hat{S}_0}(k))}{\partial \underline{r_s}^T}\right)^H \widetilde{R}_U^{-1} \frac{\partial(\widetilde{D}(k)\underline{\hat{S}_0}(k))}{\partial \underline{r_s}^T}\right\},$$
$$k = 0, 1, \ldots, N - 1, \quad (54)$$

where $\underline{\hat{S}_0}(k) = \left[\hat{S}_0^{(1)}(k), \hat{S}_0^{(2)}(k), \ldots, \hat{S}_0^{(M)}(k)\right]^T$. Note that the noise covariance matrix $\widetilde{R}_U \overset{\text{def}}{=} E\{\underline{U}(k)\underline{U}(k)^H\}$ is a diagonal matrix whose diagonal elements are $L\sigma^2$.

First, we compute

$$\frac{\partial(\widetilde{D}(k)\underline{\hat{S}_0}(k))}{\partial \underline{r_s}^T} = -\frac{j\,2\pi}{Nv} \times \widetilde{F}, \quad (55)$$

where $\widetilde{F}$ is a $P \times 2M$ matrix given by Eq. (56) above and

$$\underline{\lambda_p}^{(m)} \overset{\text{def}}{=} \left[\frac{\partial d_p^{(m)}}{\partial x_s^{(m)}}, \frac{\partial d_p^{(m)}}{\partial y_s^{(m)}}\right] = \frac{\hat{r_s}^{(m)^T} - r_p^T}{\|\underline{\hat{r_s}}^{(m)} - \underline{r_p}\|} \in \mathcal{R}^{1 \times 2}$$

$$\frac{\partial d_p^{(m)}}{\partial x_s^{(m)}} = \frac{x_s^{(m)} - x_p}{\sqrt{(x_s^{(m)} - x_p)^2 + (y_s^{(m)} - y_p)^2}}$$

$$\frac{\partial d_p^{(m)}}{\partial y_s^{(m)}} = \frac{y_s^{(m)} - y_p}{\sqrt{(x_s^{(m)} - x_p)^2 + (y_s^{(m)} - y_p)^2}}. \quad (57)$$

Thus, the entries of the Fisher information matrix with respect to $\underline{r_s}^T$ are

$$\widetilde{\mathcal{F}}(m_1, m_2) = \frac{4\pi^2}{LN^2\sigma^2 v^2}$$
$$\times \sum_{p=1}^{P}\left(a_p^{(m_1)} a_p^{(m_2)} E\left\{\hat{S}_0^{(m_1)^H}(k)\hat{S}_0^{(m_2)}(k)\right\}\right.$$
$$\times \exp\left[-\frac{j2\pi(t_p^{(m_2)} - t_p^{(m_1)})}{N}\right]$$
$$\left.\times E\left\{\underline{\lambda_p}^{(m_1)^T}\underline{\lambda_p}^{(m_2)}\right\}\right), \quad (58)$$

$$
\widetilde{F} \stackrel{\text{def}}{=}
\begin{bmatrix}
a_1^{(1)}e^{-\frac{j2\pi t_1^{(1)}}{N}}\underline{\lambda_1}^{(1)}\hat{S}_0^{(1)}(k) & a_1^{(2)}e^{-\frac{j2\pi t_1^{(2)}}{N}}\underline{\lambda_1}^{(2)}\hat{S}_0^{(2)}(k) & \dots & a_1^{(M)}e^{-\frac{j2\pi t_1^{(M)}}{N}}\underline{\lambda_1}^{(M)}\hat{S}_0^{(M)}(k) \\
a_2^{(1)}e^{-\frac{j2\pi t_2^{(1)}}{N}}\underline{\lambda_2}^{(1)}\hat{S}_0^{(1)}(k) & a_2^{(2)}e^{-\frac{j2\pi t_2^{(2)}}{N}}\underline{\lambda_2}^{(2)}\hat{S}_0^{(2)}(k) & \dots & a_2^{(M)}e^{-\frac{j2\pi t_2^{(M)}}{N}}\underline{\lambda_2}^{(M)}\hat{S}_0^{(M)}(k) \\
\vdots & \vdots & \dots & \vdots \\
a_P^{(1)}e^{-\frac{j2\pi t_P^{(1)}}{N}}\underline{\lambda_P}^{(1)}\hat{S}_0^{(1)}(k) & a_P^{(2)}e^{-\frac{j2\pi t_P^{(2)}}{N}}\underline{\lambda_P}^{(2)}\hat{S}_0^{(2)}(k) & \dots & a_P^{(M)}e^{-\frac{j2\pi t_P^{(M)}}{N}}\underline{\lambda_P}^{(M)}\hat{S}_0^{(M)}(k)
\end{bmatrix},
\tag{56}
$$

$$
\widetilde{\mathcal{F}} = \frac{4\pi^2}{LN^2\sigma^2\upsilon^2} \times \sum_{p=1}^{P}
\begin{bmatrix}
\mathcal{A}_p^{(1,1)}\widetilde{\Gamma}^{(1,1)} & \mathcal{A}_p^{(1,2)}\widetilde{\Gamma}^{(1,2)}e^{-\frac{j2\pi(t_p^{(2)}-t_p^{(1)})}{N}} \\
\mathcal{A}_p^{(2,1)}\widetilde{\Gamma}^{(2,1)}e^{-\frac{j2\pi(t_p^{(1)}-t_p^{(2)})}{N}} & \mathcal{A}_p^{(2,2)}\widetilde{\Gamma}^{(2,2)}
\end{bmatrix} \in \mathcal{R}^{4\times4}.
\tag{59}
$$

where $\hat{S}_0^{(m_1)}(k)$ and $\lambda_p^{(m_2)}$, $\forall m_1, m_2$, are assumed to be element-wise statistically independent of each other. Here m_1, m_2 indicate the row and column indices respectively. For notational convenience, we define a scalar $\mathcal{A}_p^{(m_1,m_2)} \stackrel{\text{def}}{=} a_p^{(m_1)}a_p^{(m_2)}E\left\{\hat{S}_0^{(m_1)}(k)\hat{S}_0^{(m_2)^H}(k)\right\}$ and a matrix $\widetilde{\Gamma}^{(m_1,m_2)} \stackrel{\text{def}}{=} E\left\{\underline{\lambda_p}^{(m_1)^T}\underline{\lambda_p}^{(m_2)}\right\} \in \mathcal{R}^{2\times2}$. As an example, the Fisher information matrix with two sources according to Eq. (58) is given by Eq. (59) shown on top of the next page. In employment with the matrix partitioning principles, it is easy to find that the inverse of $\widetilde{\mathcal{F}}$ has real diagonal elements. Thus, the CRLB can be defined as Eq. (40) thereby.

REFERENCES

[1] H. Krim and M. Viberg, "Two decades of array signal processing research: the parametric approach," *IEEE Signal Process. Mag.*, vol. 13, no. 4, pp. 67-94, July 1996.
[2] J. Capon, "High-resolution frequency-wavenumber spectrum analysis," *Proc. IEEE*, vol. 57, no. 8, pp. 1408-1418, Aug. 1969.
[3] R. O. Schmidt, "Multiple emitter location and signal parameter estimation," *IEEE Trans. Antennas Propagation*, vol. 34, no. 3, pp. 276-280, Mar. 1986.
[4] S. S. Reddi, "Multiple source location—a digital approach," *IEEE Trans. Aerospace Electron. Syst.*, vol. AES-15, no. 1, pp. 95-105, Jan. 1979.
[5] M. I. Miller and D. R. Fuhrmann, "Maximum-likelihood narrow-band direction finding and the EM algorithm," *IEEE Trans. Acoustics, Speech, Signal Process.*, vol. 38, no. 9, pp. 1560-1577, Sep. 1990.
[6] W. Wang, V. Srinivasan, B. Wang, and K.-C. Chua, "Coverage for target localization in wireless sensor networks," *IEEE Trans. Wireless Commun.*, vol. 7, no. 2, pp. 667-676, Feb. 2008.
[7] L. Xiao, L. J. Greenstein, and N. B. Mandayam, "Sensor-assisted localization in cellular systems," *IEEE Trans. Wireless Commun.*, vol. 6, no. 12, pp. 4244-4248, Dec. 2007.
[8] A. Boukerche, H. A. B. Oliveira, E. F. Nakamura, and A. A. F. Loureiro, "Localization systems for wireless sensor networks," *IEEE Trans. Wireless Commun.*, vol. 6, no. 6, pp. 6-12, Dec. 2007.
[9] A. J. Weiss and J. S. Picard, "Network localization with biased range measurements," *IEEE Trans. Wireless Commun.*, vol. 7, no. 1, pp. 298-304, Jan. 2008.
[10] J. C. Chen, R. E. Hudson, and K. Yao, "Maximum-likelihood source localization and unknown sensor location estimation for wideband signals in the near-field," *IEEE Trans. Signal Process.*, vol. 50, no. 8, pp. 1843-1854, Aug. 2002.
[11] ——, "Source localization of a wideband source using a randomly distributed beamforming sensor array," in *Proc. International Society Inf. Fusion*, 2001, pp. TuC1: 11-18.
[12] T. L. Tung, K. Yao, D. Chen, R. E. Hudson, and C. W. Reed, "Source localization and spatial filtering using wideband MUSIC and maximum power beamforming for multimedia applications," in *Proc. IEEE Workshop Signal Process. Syst.*, Oct. 1999, pp. 625-634.
[13] S. Valaee and P. Kabal, "Wideband array processing using a two-sided correlation transformation," *IEEE Trans. Signal Process.*, no. 1, pp. 160-172, Jan. 1995.
[14] S. Valaee, B. Champagne, and P. Kabal, "Localization of wideband signals using least-squares and total least-squares approaches," *IEEE Trans. Signal Process.*, no. 5, pp. 1213-1222, May 1999.
[15] H. Hung and M. Kaveh, "Focusing matrices for coherent signal-subspace processing," *IEEE Trans. Acoustic, Speech, Signal Process.*, no. 8, pp. 1272-1281, Aug. 1988.
[16] E. Cekli and H. A. Cirpan, "Unconditional maximum likelihood approach for localization of near-field sources: algorithm and performance analysis," *AEU International J. Electron. Commun.*, vol. 57, no. 1, pp. 9-15, Jan. 2003.
[17] I. Ziskind and M. Wax, "Maximum likelihood localization of multiple sources by alternating projection," *IEEE Trans. Acoustics, Speech, Signal Process.*, no. 10, pp. 1553-1560, Oct. 1988.
[18] K. K. Mada and H.-C. Wu, "EM algorithm for multiple wideband source localization," in *Proc. IEEE Global Telecommun. Conf.*, Nov. 2006, pp. 1-5.
[19] K. Yan, H.-C. Wu, and S. S. Iyengar, "Robustness analysis of source localization using Gaussianity measure," in *Proc. IEEE Global Telecommun. Conf.*, Nov. 2008, pp. 1-5.
[20] K. K. Mada, H.-C. Wu, and S. S. Iyengar, "Efficient and robust EM algorithm for multiple wideband source localization," *IEEE Trans. Veh. Technol.*, vol. 58, no. 6, pp. 3071-3075, July 2009.
[21] S. M. Kay, *Fundamentals of Statistical Signal Processing, Estimation Theory*. Prentice-Hall, 1993.
[22] A. Renaux, P. Forster, E. Boyer, and P. Larzabal, "Unconditional maximum likelihood performance at finite number of samples and high signal-to-noise ratio," *IEEE Trans. Signal Process.*, vol. 55, no. 5, pp. 2258-2364, May 2007.
[23] N. Menemenlis and C. D. Charalambous, "An Edgeworth series expansion for multipath fading channel densities," in *Proc. IEEE Conf. Decision Control*, vol. 4, Dec. 2002, pp. 4030-4035.
[24] H. Cramer, *Random Variables and Probability Distributions*. Cambridge University Press, 1970.
[25] M. Hinich, "Testing for Gaussianity and linearity of a stationary time series," *J. Time-Series Analysis*, vol. 3, no. 3, pp. 169-176, 1982.
[26] A. M. Zoubir and D. R. Iskander, "Bootstrapping bispectra: an application to testing for departure from Gaussianity of stationary signals," *IEEE Trans. Signal Process.*, vol. 47, no. 3, pp. 880-884, Mar. 1999.
[27] H.-C. Wu, "Blind source separation using information measures in the time and frequency domains," Ph.D. thesis, Department of Electrical and Computer Engineering, University of Florida, Gainesville, FL, USA, 1999.
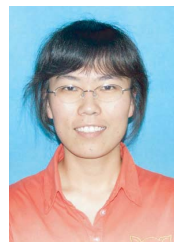
Kun Yan received the B.S.E.E. and M.S. degrees from Xidian University, Shaanxi, China, in 2004 and 2008, respectively. She is currently working toward the Ph.D. degree in electrical and computer engineering, Louisiana State University, Baton Rouge, Louisiana, USA. Her research interests are in the area of digital communications as well as digital and statistical signal processing.

Hsiao-Chun Wu (M'00-SM'05) received a B. S. E. E. degree from National Cheng Kung University, Taiwan, in 1990, and the M. S. and Ph. D. degrees in electrical and computer engineering from University of Florida, Gainesville, in 1993 and 1999 respectively. From March 1999 to January 2001, he had worked for Motorola Personal Communications Sector Research Labs as a Senior Electrical Engineer. Since January 2001, he has joined the faculty in Department of Electrical and Computer Engineering, Louisiana State University, Baton Rouge, Louisiana, USA. From July to August 2007, Dr. Wu had been a visiting assistant professor at Television and Networks Transmission Group, Communications Research Centre, Ottawa, Canada. From August to December 2008, he was a visiting associate professor at Department of Electrical Engineering, Stanford University, California, USA.

Dr. Wu has published more than 120 peer-refereed technical journal and conference articles in electrical and computer engineering. His research interests include the areas of wireless communications and signal processing. Dr. Wu is an IEEE Senior Member and an IEEE Distinguished Lecturer. He currently serves as an Associate Editor for IEEE TRANSACTIONS ON BROADCASTING, IEEE SIGNAL PROCESSING LETTERS, IEEE COMMUNICATIONS MAGAZINE, *International Journal of Computers and Electrical Engineering*, *Journal of Information Processing Systems*, *Physical Communication*, and *Journal of the Franklin Institute*. He used to serve as an Associate Editor for IEEE TRANSACTIONS ON VEHICULAR TECHNOLOGY. He has also served for numerous textbooks, IEEE/ACM conferences and journals as the technical committee, symposium chair, track chair, or the reviewer in signal processing, communications, circuits and computers.

S. S. Iyengar (Fellow, IEEE) is the Chairman and Roy Paul Daniels Chaired Professor of Computer Science at Louisiana State University, Baton Rouge, and is also the Chaired Professor at various institutions around the world. His publications include six textbooks, five edited books and over 380 research papers. His research interests include high-performance algorithms, data structures, sensor fusion, data mining, and intelligent systems. He is a world class expert in computational aspects of Sensor Networks, Data Structures, and Algorithms for various distributed applications. His techniques have been used by various federal agencies (NRL, ORNL, NASA) for their projects. His work has been cited very extensively by researchers and scientists around the world. He is an SIAM Distinguished lecturer/ ACM National Lecturer/ IEEE Distinguished Scientist. He is a Fellow of IEEE, Fellow of ACM, Fellow of AAAS and Fellow of SDPS. He is a recipient of IEEE awards, best paper awards, the Distinguished Alumnus award of the Indian Institute of Science, Bangalore and other awards.

He has served as the editor of several IEEE journals and is the founding editor-in-chief of the International Journal of Distributed Sensor Networks. His research has been funded by National Science Foundation (NSF), Defense Advanced Research Projects Agency (DARPA), Multi-University Research Initiative (MURI Program), Office of Naval Research (ONR), Department of Energy/OakRidge national Laboraoty (DOE/ORNL), Naval Research Laboratory (NRL), National Aeronautics and Space Administration (NASA), US Army Research Office (URO) and various state agencies and companies. He has served on US National Science Foundation and National Institute of Health Panels to review proposals in various aspects of computational science and has been involved as and external evaluator (ABET-accreditation) for several computer science and Engineering departments. Dr. Iyengar had 40 doctoral students under his supervision and the legacy of these students can be seen in prestigious Laboratories (JPL, Oak Ridge National Lab, Los Alamos National Lab, Naval Research Lab) and universities round the world. He has been the program Chairman of various international conferences and has given more than 50 keynote talks at international conferences.